Study of Hydrogen-Bonded Blend of Polylactide with Biodegradable Hyperbranched Poly(ester amide)

Ying Lin,[†,‡] Kun-Yu Zhang,[†,‡] Zhong-Min Dong,[†,‡] Li-Song Dong,[†] and Yue-Sheng Li*[,†]

State Key Laboratory of Polymer Physics and Chemistry, Changchun Institute of Applied Chemistry, Chinese Academy of Sciences, Changchun 130022, China, and Graduate School of the Chinese Academy of Sciences

Received April 30, 2007; Revised Manuscript Received June 2, 2007

ABSTRACT: Polylactide (PLA) was melt blended with a biodegradable hyperbranched poly(ester amide) (HBP) to enhance its flexibility and toughness without sacrificing comprehensive performance. The advantage of using HBP was due to its unique spherical shape, low melt viscosity, and abundant functional end groups together with its easy access. Rheological measurement showed that blending PLA with as little as 2.5% HBP resulted in a 40% reduction of melt viscosity. The glass transition temperature (T_g) of PLA in the blends decreased slightly with the increase of HBP content, indicating partial miscibility which resulted from intermolecular interactions via H-bonding. The H-bonding involving C═O of PLA with OH and NH of HBP was evidenced by FTIR analysis for the first time. The HBP component, as a heterogeneous nucleating agent, accelerated the crystallization rate of PLA. Remarkably, with the increase of HBP content, the elongation at break of PLA blends dramatically increased without severe loss in tensile strength, even the tensile strength increased within 10% content of HBP. The stress−strain curves and the SEM photos of impact-fractured surface showed the material changed from brittle to ductile failure with the addition of HBP. Reasonable interfacial adhesion via H-bonding and finely dispersed particulate structure of HBP in PLA were proposed to be responsible for the improved mechanical properties.

1. Introduction

Polylactide (PLA) has been intensively studied and widely used for biomedical materials because of its high biocompatibility and good biodegradability in the human body as well as in the earth's environment.[1] However, PLA fall short of the required properties for potential applications. Major disadvantages of PLA are its inherent brittleness and low toughness.[2] Nevertheless, the flexibility and toughness of PLA can be improved by modifying its physical properties through several approaches including copolymerization and blending.[3] As blending is a simpler and more economic way compared with copolymer synthesis, much attention has been focused on the blends of PLA with various polymers, for example, poly(ϵ-caprolactone),[4] poly(ethylene glycol),[5] poly(propylene glycol),[6] poly(hydroxy butyrate),[7] and other polymers.[8] Various low molecular weight compounds and oligomers have also been investigated as potential plasticizers for PLA.[9] Blending PLA with low molecular weight compounds can drastically lower the T_g of PLA, thus creating homogeneous and flexible materials. However, with long-term use of the materials, the plasticizers have a tendency to migrate to the surface, which would cause embrittlement. Furthermore, the too low T_g may affect the processing and molding of final products.[9] Whereas, when relatively high molecular weight polymers were blended with PLA, the aforementioned problem could be prevented, but the desired properties were not obtained due to their thermodynamically immiscibility and phase segregation.[4−8] Even though the toughness increases, a drastic sacrifice of processability and tensile strength would be induced.

Hyperbranched polymers have received extraordinary attention in recent years.[10] Compared to dendrimers, hyperbranched polymers can be produced in industrial quantities at low cost while still inheriting many of the fascinating properties of dendrimers. Therefore, hyperbranched polymers have great potential for a wide range of applications in materials, especially for industrial use. Since highly branched molecules do not undergo chain entanglements, they provide materials with poor mechanical strength, as predicted by Flory in 1952.[11] Thus, unlike linear polymers, hyperbranched polymers rarely have sufficient strength to be useful as fibers, rubbers, and plastics. In contrast, hyperbranched polymers have higher solubility and miscibility with other materials because of their low secondary attractive forces. Besides, the globular shape of hyperbranched polymers results in low hydrodynamic volume and low viscosity. As a result, numerous applications have been suggested for hyperbranched polymers, e.g., rheology modifiers,[12] surface modification agents,[13] toughners for epoxy-based composites,[14] and coating.[15] As early as 1990, hyperbranched polymer was first used as an additive by Kim and Webster.[12a,b] It was demonstrated that hyperbranched polyphenylene could reduce the melt viscosity for polystyrene processing. As a surface modification agent, hyperbranched polymer had been shown to eliminate melt fracture and sharkskin of polyethylene and improve the surface properties of final products.[13] The research of Månson's group indicates that Boltorn hyperbranched polyesters can act as the outstanding toughners in epoxy resins by chemical bonds and produce desirable processing characteristic, without influencing the thermomechanical property of the resin system.[14a−e]

Herein, hyperbranched polymer was employed to act as modifier to PLA. Because of the unique three-dimensional globular structure, hyperbranched polymer results in different dispersion phase size and stereo hindrance from the linear polymer. Furthermore, the abundance of hydroxyl end groups attached to hyperbranched polymer may have some interactions with PLA, presumably via H-bonding. As suggested by the

* Corresponding author. E-mail: ysli@ciac.jl.cn.
† State Key Laboratory of Polymer Physics and Chemistry.
‡ Graduate School of the Chinese Academy of Sciences.

10.1021/ma070989a CCC: $37.00
Published on Web 07/21/2007

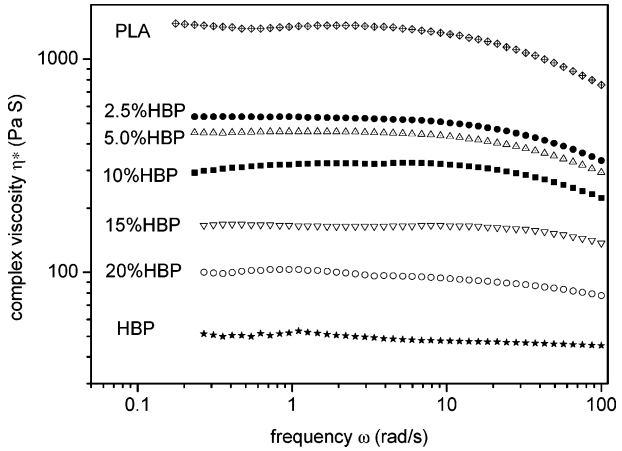

Figure 1. Effect of HBP concentration on the complex viscosity of PLA/HBP blend (T = 175 °C, frequency sweep 0.1−100 rad/s).

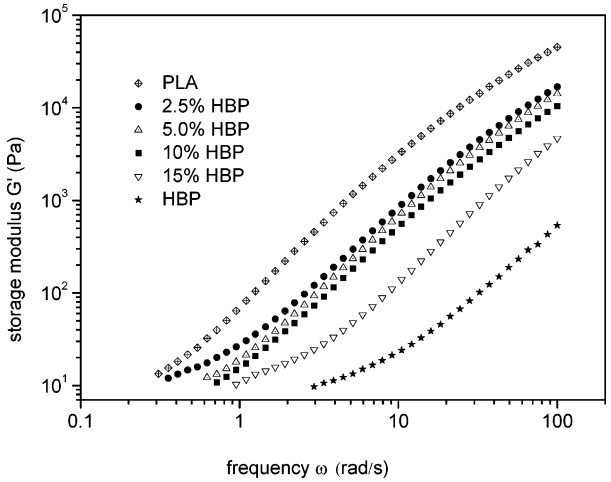

Figure 2. Effect of HBP concentration on the storage modulus G' of PLA/HBP blend (T = 175 °C, frequency sweep 0.1−100 rad/s); data below 10 Pa were omitted due to the low signal-to-noise ratio.

literature, the H-bonding can improve interfacial adhesion of polymer composites.[16] Thus, it is quite reasonable to expect that the incorporation of hyperbranched polymer into PLA may bring about either improved toughness or increased strength in comparison with unmodified PLA. In previous studies,[17] we reported on the facile synthesis of hyperbranched poly(ester amide)s from commercial available monomers via the one-pot procedure. Characterization studies underlined the properties of hyperbranched poly(ester amide), such as high solubility, low solution and melt viscosity, good thermal stability, and biodegradability.[18] Furthermore, the inability to crystallize of hyperbranched polymer due to the highly branched architecture makes them more attractive. On this basis, PLA have been modified with hyperbranched poly(ester amide) to overcome the brittleness and improve general performance in this paper. The tensile mechanical behavior of the blend was evaluated, and the toughening effect of the hyperbranched polymer on PLA was observed. H-bonding between PLA and HBP was first evidenced by FT-IR analysis. The rheological and thermal properties were studied in order to observe whether favorable effects on the processability and crystallization would accompany toughness.

2. Experimental Part

Materials. The PLA used in this study was purchased from Mitsui Chemicals (Japan) and was prepared mainly from L-lactic acid. The PLA exhibits a number-average molecular weight ($\bar{M}_n$) of 80 kDa, polydispersity index of 1.27 (SEC analysis), and a T_g and a melting temperature (T_m) of 64.4 and 159.8 °C (DSC analysis), respectively. The hyperbranched poly(ester amide) was prepared according to the procedure described previously.[17a] For convenience, hyperbranched poly(ester amide) is denoted as HBP in the following discussion. The HBP exhibits a $\bar{M}_n$ of 4.2 kDa, polydispersity index of 3.01, and T_g of 27.2 °C. The chemical structure of HBP is presented in Scheme 1.

Blend Preparation. PLA was mechanically mixed with HBP from 2.5 to 20% (w/w). Addition of more than 20% of HBP is not reasonable considering application aspects. Prior to blending, PLA and HBP were dried in vacuo at 90 and 60 °C for 24 h, respectively. Melt blends were prepared by using a Haake batch intensive mixer (Haake Rheomix 600, Germany) with a batch volume of 50 mL. Polymers were mixed at a screw speed of 30 rpm for 5 min at 175 °C. The torque was continuously monitored during the whole mixing process. Also, the neat PLA was subjected to the mixing treatment so as to have the same thermal history as the blends.

Characterizations. For the study of rheological behaviors, the samples were pressed into 1 mm thick plates at 180 °C. The

Scheme 1. Chemical Structure Presentation of Hyperbranched Poly(ester amide) (HBP) Used in This Study

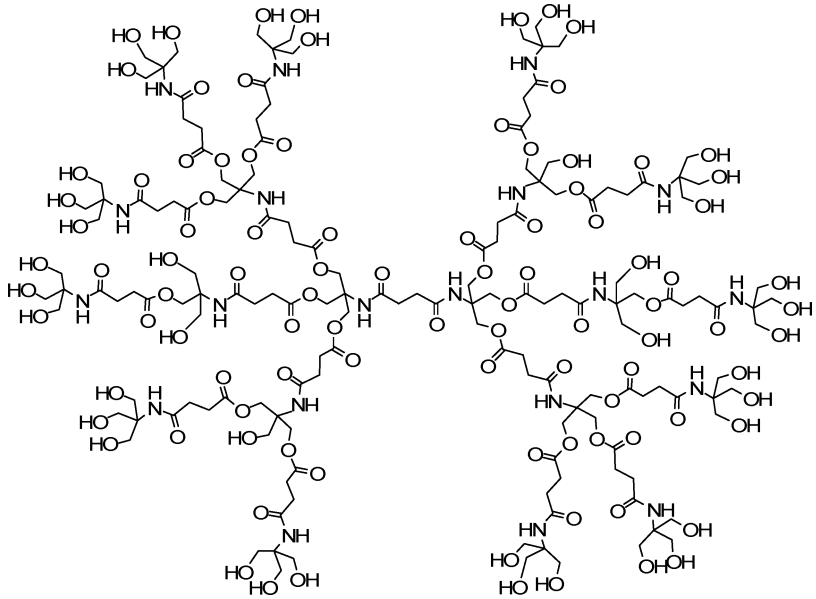

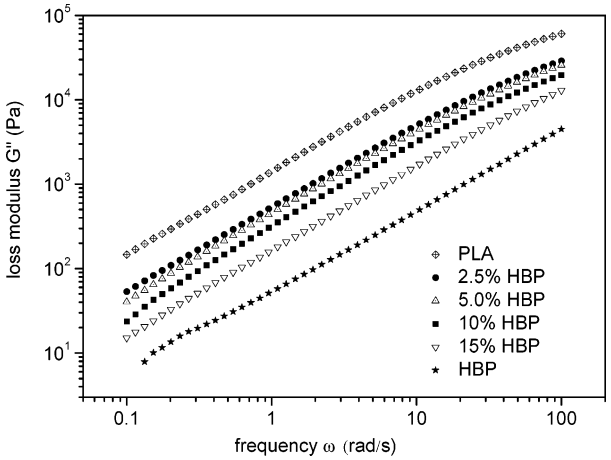

Figure 3. Effect of HBP concentration on the loss modulus G'' of PLA/HBP blend (T = 175 °C, frequency sweep 0.1−100 rad/s).

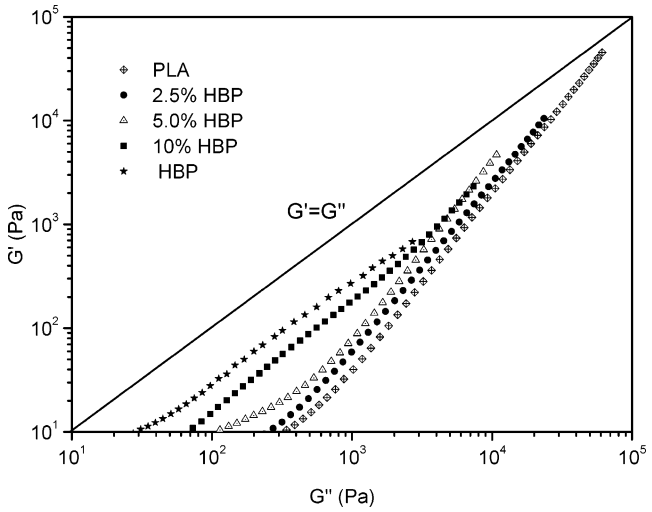

Figure 4. Storage modulus G' vs loss modulus G'' of PLA/HBP blend.

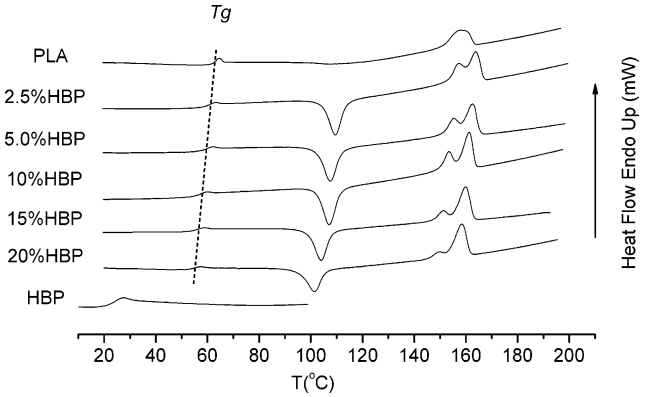

Figure 5. DSC traces of PLA blended with various HBP concentrations.

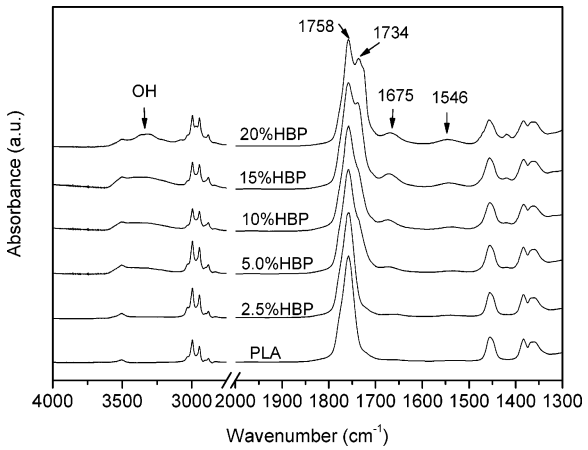

Figure 6. FTIR spectra for PLA/HBP blends with various HBP contents. The peak at 1734 cm^{-1} indicated the formation of H-bonding.

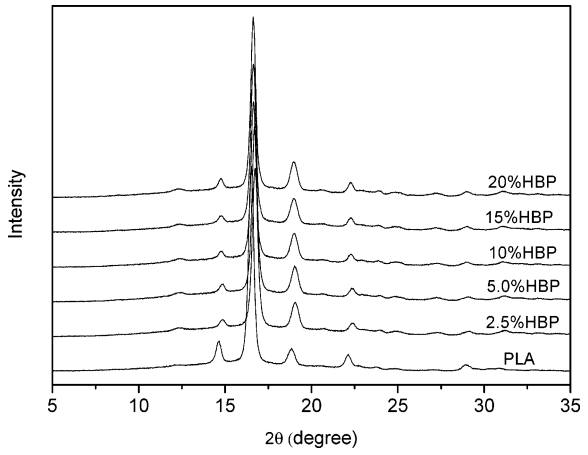

Figure 7. WAXD patterns of PLA and its various HBP blends.

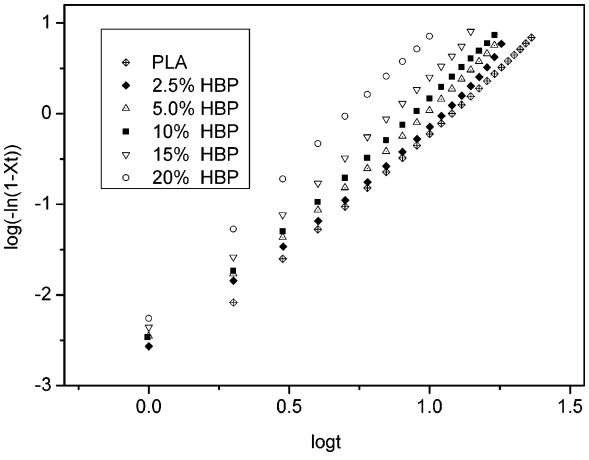

Figure 8. Effect of HBP concentration on isothermal crystallization of PLA at 112 °C.

rheological measurements were carried out on a PHYSICA MCR 300 instrument (Stuttgart, Germany). Frequency sweep for the samples was carried out under nitrogen at 175 °C using 25 mm plate−plate geometry, and the sample gap was set as 0.5 mm. A strain sweep test was initially conducted to determine the linear viscoelastic region of the materials. The strain and angular frequency range used during testing were 5% and 0.1−100 rad/s, respectively. MCR300 software was used to acquire data.

Differential scanning calorimetry (DSC) measurements were performed on a Perkin-Elmer Pyris 1 DSC instrument under a N_2 atmosphere. The samples were heated from 0 to 150 °C and cooled to 0 °C at a rate of 20 °C/min. The T_m and the value of fusion heat (ΔH_m) were taken from the second heating curve to minimize different thermal history effects. The degree of crystallinity of the samples were calculated from the ratio of their enthalpy of fusion to the enthalpy of fusion of the PLA crystal ΔH_m^0 (we used a value of 96 J/g).[19] Isothermal crystallization behaviors of PLA/HBP blends were also evaluated using DSC by premelting blends at 200 °C for 5 min to completely eliminate any possible crystallinity or residual stresses in the sample and then rapidly cooling to the designed

Table 1. Thermal Parameters of PLA/HBP Blends with Various HBP Contents

HBP ratio (%)	T_g (°C)	T_{cc} (°C)	T_{m1} (°C)	T_{m2} (°C)	ΔH_c[a] (J/g)	ΔH_m[a] (J/g)	X_c[b] (%)
0	64.45	112.8	159.8		5.48	19.35	20.16
2.5	63.22	109.8	157.1	163.7	26.68	29.82	31.06
5.0	61.86	107.6	155.4	163.7	28.01	32.30	33.65
10	59.69	106.9	153.4	161.3	29.97	33.50	34.90
15	57.98	104.1	151.2	159.7	27.35	29.46	30.69
20	56.62	101.5	149.3	158.2	19.68	25.87	26.95

[a] Data corrected for the percentage of PLA in the blend. [b] $\Delta H_m$for 100% crystalline PLA equals 96 J/g.

crystallization temperature and holding there for 30 min to allow crystallization from the quiescent melt. The temperature was ramped back up to 200 °C with a heating rate of 10 °C/min to probe the melting point after crystallization. The exothermic curves of heat flow as a function of time were recorded, and relative crystallinity was expressed as the ratio of peak areas at time to that at the end of crystallization. Wide-angle X-ray diffraction (WAXD) experiments were carried out by the use of Rigaku D/Max-II B X-ray diffractometer with a Cu anode (Cu $K\alpha_1 = 1.5406$ Å). The measurements were operated at 40 kV and 20 mA from 2° to 40° at a 2θ scan rate of 4 °C/min.

Tensile tests were performed on a 8.9 kN, screw-driven universal testing machine (Instron 1211, Canton, MA) equipped with a 10 kN electronic load cell and mechanical grips. The tests were conducted at room temperature using a cross-head rate of 5 mm/min. All tests were carried out according to the ASTM standard, and the data reported were the mean and standard deviation from five determinations.

Infrared spectroscopic measurements were recorded with a Bruker Vertex 70 FTIR spectrophotometer, and 50 scans were collected with a spectral resolution of 1 cm^{-1}. The 1,4-dioxane solution containing the blend samples were cast onto a conventional KBr disk and allowed to evaporate at room temperature followed by vacuum drying at 50 °C for 24 h. The films used in this study were sufficiently thin to obey the Beer−Lambert law.

Polar optical microscopy (POM) studies were carried out with a Microphoto (Linkam TM 600) in conjunction with a hot stage. The samples of PLA and the PLA/HBP blends were prepared by cutting small pieces from prepared films. Samples weighing 5 mg were melted on glass slides with coverslips to form thin films 20−50 μm thick. The specimens were heated to 180 °C on a hot stage and held at that temperature for 3 min and then quickly cooled to 120 °C at a rate of 40 °C/min. The POM observation was carried out as soon as the sample was cooled to 120 °C. The hot stage was calibrated with a melting point standard to 0.2 °C accuracy. In addition, photographs were taken by a digital camera.

Scanning electron microscopy (SEM) was observed with a XL30 ESEM FEG (FEI Co.). The phase morphology of blend was assessed by observation of microtomed surfaces using SEM. The microtoming was carried out at room temperature using a knife. To obtain a better observation of the phase structure, the microtomed surfaces were etched in methanol for 3 h at room temperature in order to selectively dissolve the HBP phase, rinsed with MeOH and water, followed by vacuum drying at 50 °C for 5 h. Then the specimen was mounted on an aluminum stub using a conductive paint and finally sputtered with gold prior to fractographic examination. Fracture surfaces from notched impact test samples were also examined with SEM, but no etching was carried out.

3. Results and Discussion

Rheological Behavior. During the mixing procedure, a dramatic reduction of final torque value upon incorporating HBP into PLA was observed, and the appearance of blend seems to be smoother than neat PLA. The processing aid function of HBP was investigated further by determining the HBP concentration dependence of the blend viscosity. Figure 1 exhibits the complex viscosities η^* of PLA and its HBP blends vs frequency. From Figure 1, we found that a significant drop in the blend viscosity occurred immediately on addition of HBP, even at levels as low as 2.5%. In comparison with neat PLA, the complex viscosity η^* of the blend with 2.5% HBP lowered to about 40% of original value. Further increase of HBP led to a continuous decrease η^* of blends. As shown in Figure 1, the value of complex viscosity was rarely dependent on the frequency in the range studied, exhibiting a Newtonian behavior of the melt. The measured complex melt viscosities of PLA/HBP blends

Scheme 2. Schematic Illustration of Intermolecular H-Bonding between HBP and PLA

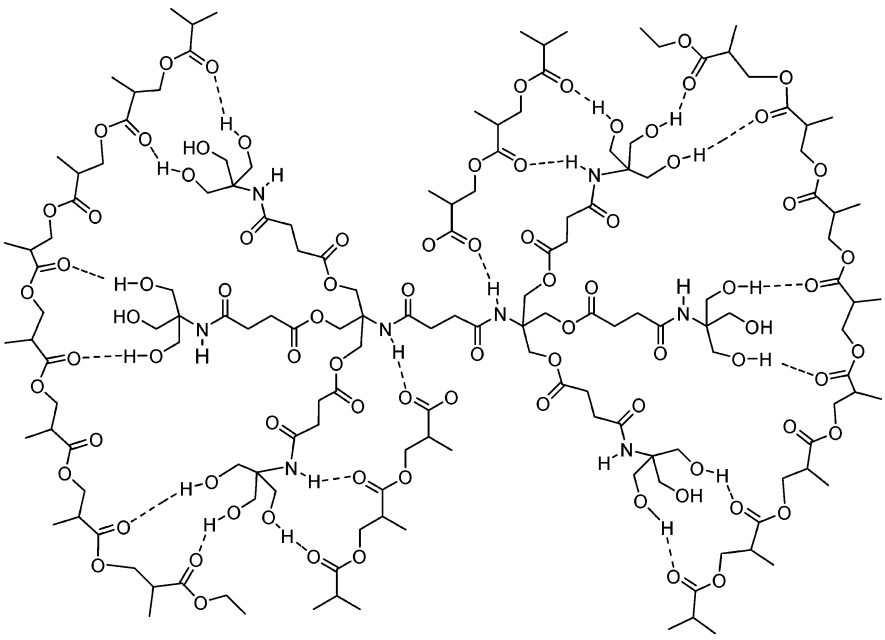

Table 2. Fraction of the H-Bonded Carbonyl Group for PLA Blended with Various Hyperbranched Polymers with Different Compositions

	free C═O			H-bonded C═O			
PLA/HBP	ν (cm^{-1})	$W_{1/2}$ (cm^{-1})	A_f (%)	ν (cm^{-1})	$W_{1/2}$ (cm^{-1})	A_b (%)	f_b (%)
2.5/97.5	1759.6	28.1	84.2	1736.6	31.5	15.8	11.1
5.0/95	1759.2	29.0	77.5	1736.1	28.9	22.5	16.7
10/90	1759.3	30.1	71.7	1735.0	27.8	28.3	20.7
15/85	1758.7	27.2	62.0	1733.5	34.3	38.0	28.9
20/80	1758.6	24.3	53.2	1732.2	26.7	46.8	36.9

Table 3. Kinetic Crystallization Parameters of PLA with Various HBP Concentrations at Isothermally Crystallized Temperature 112 °C

HBP ratio (%)	N	K (10^{-3} min^{-1})	$t_{1/2}$ (min)
0	2.68	1.44	10.01
2.5	2.68	1.68	9.39
5.0	2.70	2.39	8.17
10	2.77	2.50	7.58
15	2.93	3.06	6.37
20	3.20	5.67	4.49

were significantly lower than predicted by the additive effect of the linear mixing rule:

$$\eta^*_{1,2} = \phi_1\eta^*_1 + \phi_2\eta^*_2 \quad (1)$$

where ϕ_1 and ϕ_2 are the weight ratio of the components 1 and 2, respectively, and η^*_1 and η^*_2 are the viscosities of the two components.[12d] For instance, the experimental value for η^* of the blend with 10% HBP at 1.0 rad/s was 320 Pa s, while the predicated value was 1292 Pa s. Such large reduction has already been observed for other blends.[12,16b] Several factors might be responsible for the decreased melt viscosity. First, a structural change of the PLA matrix would be induced due to the incorporation of HBP. It was reasonable to expect the globular-shaped hyperbranched polymers to disrupt the copious entanglements of linear chains by physically separating them. As a result, introducing HBP to PLA will result in fewer entanglements. Second, the free volume of the system will become larger with the addition of HBP due to its abundant end groups. The free volume plays a major role in the internal friction forces experienced by the units involved in motion. With the increase of free volume, the internal friction of molecules is decreased, and thus the melt viscosity is markedly decreasing. Third, it was the result of the large disparity between the intrinsic viscosity of PLA and HBP. PLA has an intrinsic viscosity 20 times greater than that of HBP. Also, there is an inherently nonlinear relationship between intrinsic and complex viscosity.[12e] For example, the Lyons−Tobolsky equation has an exponential relationship between these two viscosities. Therefore, replacing just a small amount of PLA with HBP can result in large reductions in complex viscosity.

It is well-known that the complex viscosity can be separated into the storage modulus G' and the loss modulus G''.[12d] The elastic part of the complex melt viscosity is represented by G', while the viscous part is described by G''. Plotting G' and G'' against frequency, the decrease trend is similar to that for η^*, as shown in Figures 2 and 3. The effect of the HBP component on the rheological behavior of the blends can be seen well from a plot of G' vs G'' (Figure 4), which is termed a Cole−Cole plot. A Cole−Cole plot is useful for comparing the differences in elastic and viscous properties in low frequencies, where the linear viscoelastic data are most sensitive to differences in structure. The intersection ($G' = G''$) determines the transition from more viscous behavior ($G' < G''$) to more elastic behavior ($G' > G''$). Although the PLA and all blends exhibited a predominantly viscous behavior at 175 °C rather than an elastic behavior, the elastic part was increasing with an increase of the HBP in the blend, especially in low frequencies. A reason for this effect could be related to the molecular interaction between PLA and HBP, i.e., hydrogen bonding. More details about it will be addressed in the following section.

Miscibility and Hydrogen Bonding. DSC was employed to assess the miscibility of the polymer blend by measuring the T_g of the blend composition. Figure 5 shows the second heating scans of DSC thermogram for HBP, PLA, and various PLA/HBP blends at a rate of 20 °C/min. Table 1 summarizes the results obtained from this heating run for all the samples. All blends exhibited only one single T_g, which might suggest that HBP was miscible with PLA at all concentrations. As a general trend, the T_g of the blends shifted slightly to lower temperature with the increase of HBP content in blend, suggesting that HBP acted as a plasticizer for PLA in a way. Different equations have been proposed to predict variations of T_g for polymer blends as a function of composition. The most popular equation is the Fox equation[20] as follows:

$$\frac{1}{T_g} = \frac{W_1}{T_{g1}} + \frac{W_2}{T_{g2}} \quad (2)$$

where W is the weight fraction, whose subscripts "1" and "2" indicated polymer 1 and 2, respectively. This equation is applicable to binary blend systems that are completely miscible. However, the observed value of T_g of 59.69 °C (10% HBP) and 56.62 °C (20% HBP) were slightly higher than that calcd from the Fox equation (calcd: $T_{g(10\%\ HBP)}$ = 56.66 °C, $T_{g(20\%\ HBP)}$ = 52.00 °C). The deviation from the Fox mixing rule was thought to arise from partial miscibility of the blend system. SEM data presented later also show that HBP is only partially miscible with PLA, especially at higher concentrations. Partially miscibility would suggest that there should be two T_g's in these blends. However, the T_g attributable to HBP was not detected, maybe due to the relatively low concentration of HBP in blend and the limitations of the DSC technique. As we know, the DSC equipment is not sensitive to such a small enthalpy at a slow scanning rate. As a result, although all blends exhibited only single T_g, the blends were inferred as partially miscible.

There was a great mismatch between PLA and HBP in the terms of molecular structure and polarity. Why did the blend exhibit partially miscibility, and did the miscibility arise from the molecular interaction between PLA and HBP, i.e., hydrogen bonding? We employed the FTIR technique to verify this specific interaction between polymers because of its sensitivity to H-bonding formation.[21] Scheme 2 gives a schematic illustration of intermolecular H-bonding between HBP and PLA. As shown in Scheme 2, the H-bonding involves C═O groups of PLA, often regarded as H-bonding acceptor, together with OH and NH groups of HBP, usually regarded as H-bonding donor. The abundance of terminal OH groups of HBP provided a favorable condition for the formation of H-bonding. Figure 6 shows scale-expanded infrared spectra recorded at room temperature for pure PLA and its blends with various HBP contents.

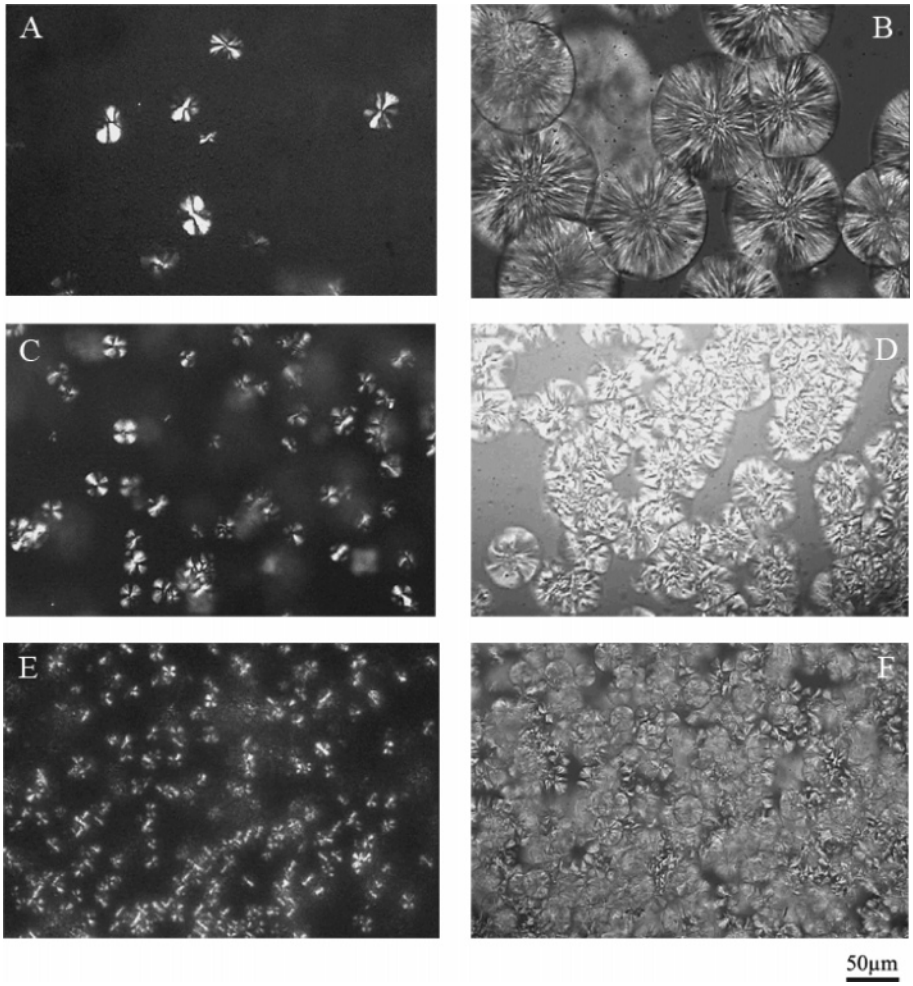

Figure 9. Polarized optical microscopy images of neat PLA (A, B), 10% HBP (C, D), and 20% HBP (E, F) isothermally crystallized from quiescent melt at 120 °C for 10 min (A, C, E) and 30 min (B, D, F).

All the spectra had been normalized using the area of the C═O stretching region (1800−1700 cm^{-1}) of the samples for an easier visualization. The intensity of the signal of the hydroxyl groups (in the region 3500−3100 cm^{-1}) increased gradually with the increase of HBP content. Meanwhile, two new absorption bands centered at 1675 and 1546 cm^{-1}, which were assigned to the C═O stretching and N−H bending mode for amide group in HBP, appeared upon adding the HBP, and the intensity increased with increasing the HBP content. Remarkably, the narrow and symmetrical peak centered at 1758 cm^{-1}, characteristic of the C═O stretching mode of ester in PLA, became broader and eventually split into two bands, which can be fitted well to the Gaussian function. The shoulder in the vicinity of 1734 cm^{-1} was more and more distinguishable with the increase of HBP content. It indicated that the peak at lower frequency should be characteristic of hydrogen-bonded carbonyl, since the hydrogen bond weakened the force constant of C═O double bond. The fraction of the H-bonded carbonyl group can be calculated by the following equation:[22]

$$f_b^{C=O} = \frac{A_b/1.5}{A_b/1.5 + A_f} \quad (3)$$

where A_f and A_b are peak areas corresponding to the free and H-bonded carbonyl groups, respectively. The conversion coefficient 1.5 is the ratio of these two bands in an ester group.[22] Results from curve fitting summarized in Table 2 indicated that the H-bonded fraction of the carbonyl group increased with the increasing content of HBP, as a H-bonding donor polymer. In the early literature,[16] H-bonding between hyperbranched polymer and its blend has been discussed widely but never evidenced. To our best knowledge, it is the first time to demonstrate the existence of H-bonding between hyperbranched polymer and its blend by experimental techniques.

Crystallization and Melting Behavior Analysis. Crystallization of PLA is of great technological importance due to the mechanical properties and degradation rate imparted. Therefore, the influence of HBP on crystallization behavior of PLA was investigated. As reflected by Figure 5, all samples showed exothermic peaks attributed to the cold crystallization during the temperature increase of DSC scanning. The corresponding temperature is known as the cold crystallization temperature (T_{cc}). Neat PLA represented a tiny broad exothermic peak at 112 °C, indicating a rather low cold crystallization capability.[8d] However, in the case of the blend this peak was sharper and appeared at lower temperature. It suggested that the incorporation of HBP enhanced crystalline ability of PLA. As already stated, the incorporation of globular-shaped hyperbranched polymer resulted in larger free volume of PLA chains than neat PLA. Consequently, HBP improved the mobility of PLA segment, and thus the crystalline ability of PLA was enhanced.

In parallel with the shift in T_{cc}, the T_m of PLA component was also gradually shifted down with increasing the HBP content. Interestingly, the melting peak had a transition from

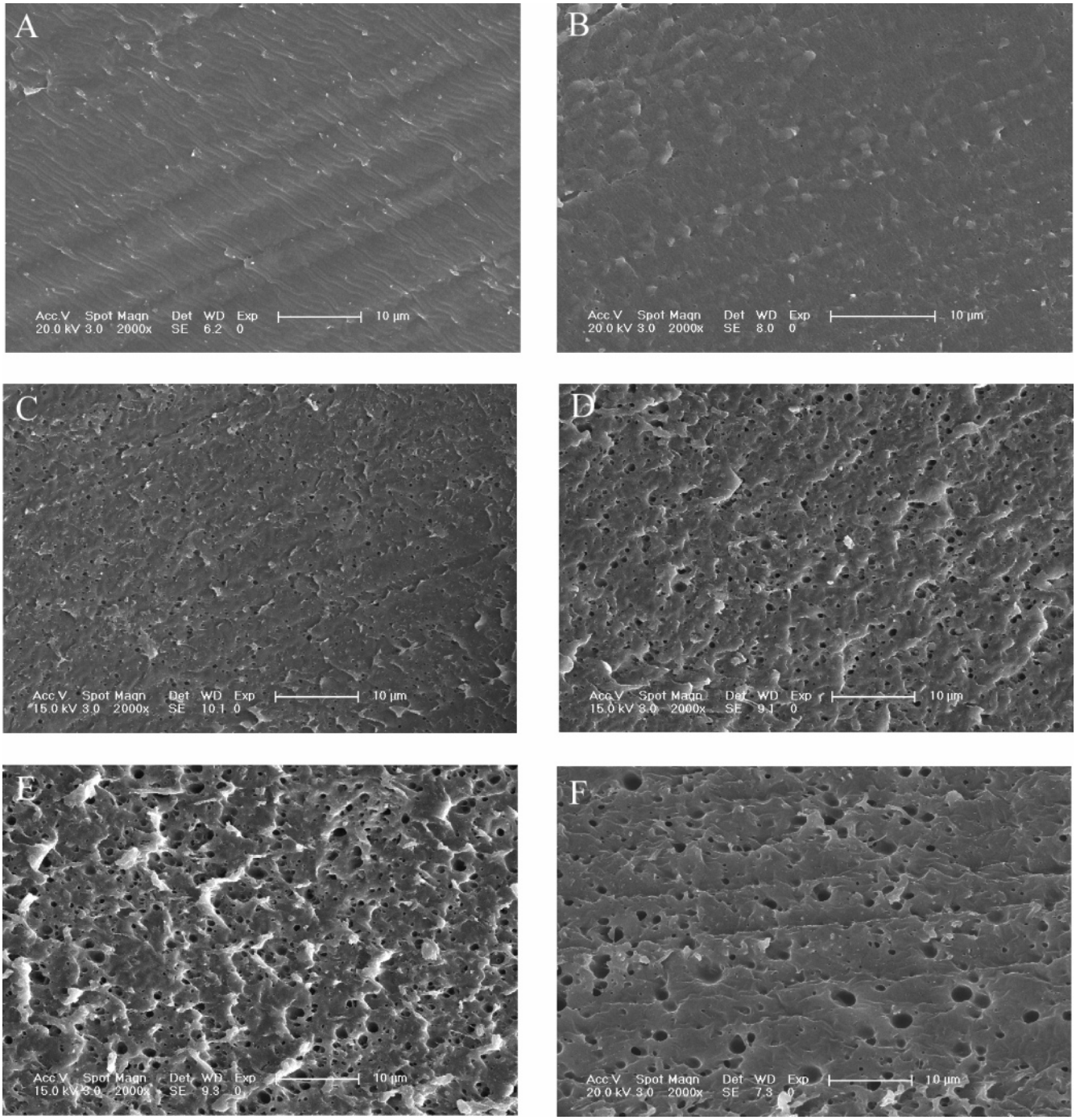

Figure 10. SEM photos of microtomed surface of PLA/HBP blend with various PLA/HBP weight compositions of (A) 100/0, (B) 97.5/2.5, (C) 95/5, (D) 90/10, (E) 85/15, and (F) 80/20 (magnification ×2000).

single peak to two separate peaks. The bimodal peak may be a result of the polymorphic crystalline transition in view of PLA can display three different kinds of crystal modification, i.e., α, β, and γ.[23] However, it was reported from the literature that the β and γ crystal forms can only appear for PLA upon hot drawing to high draw ratios[23a] and stroking,[23b] respectively. Considering the form condition of β and γ modifications, the crystal state we got can only be α crystal. To demonstrate it, the WAXD patterns of PLA and its HBP blends are given in Figure 7. The characteristic reflection peaks of α crystal PLA kept almost the same position regardless of the composition variations, although the intensity had some changes. Consequently, the bimodal melting peaks must result from another reason. It was induced during the slow DSC scans when the less perfect crystals had enough time to melt and reorganize into crystals with higher structural perfection and remelt at higher temperature. A similar phenomenon was also reported by other PLA blends.[7e,8d,19] In this work, with increasing HBP content, the peak at the lower temperature faded while the peak at the higher temperature became dominant, indicating that more perfect crystals formed. Usually, imperfect crystals containing cracks or microcrystals are typical of a brittle matrix, whereas perfect crystals may contribute to the improved toughness.[24] Crystallinities of the blends estimated from the DSC thermograms are also presented in Table 1. From the data listed in Table 1, we found that the crystallinity of PLA markedly

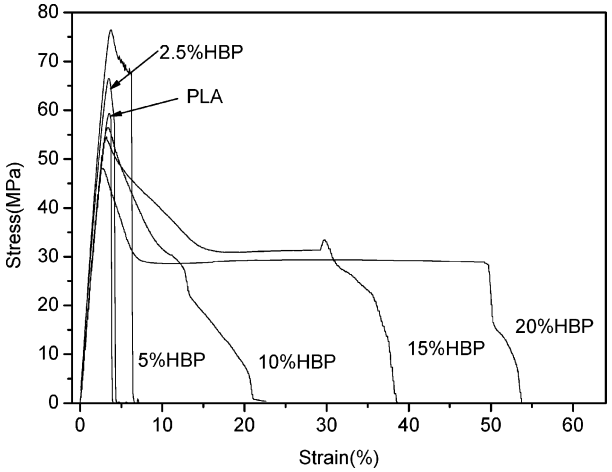

Figure 11. Tensile stress−strain curves of the blends with different HBP contents.

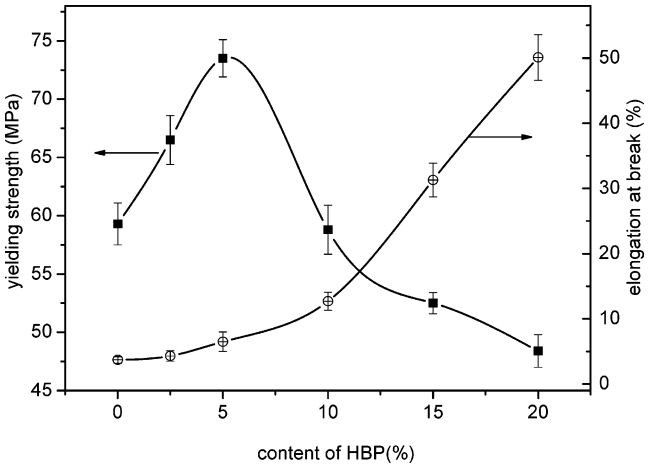

Figure 12. Mechanical properties of PLA with various HBP concentrations.

increased from 20.16% for pure PLA to 31.06% for blend with 2.5% HBP and further increased to 34.90% for blend with 10% HBP, which was in agreement with the enhanced cold crystallization capacity mentioned above. However, when 20% HBP was incorporated, the crystallinity of PLA was decreased to 26.95%. The reason can be explained by the dilution effect of the amorphous phase of HBP on the system.

Isothermal Crystallization Kinetics. Most PLA are finished to final products by melt compounding in extruders or by injection molding process; therefore, fast crystallization is a very important property of PLA. It was addressed above that HBP improved the crystalline ability of PLA. To further demonstrate it, the crystallization rate of neat PLA and the blends was investigated using isothermal crystallization kinetics. To describe it, the classical Avrami equation was used:[25]

$$1 - X_t = \exp(-kt^n) \tag{4}$$

where X_t is the amount of crystallized material or the conversion degree to crystalline phase, n is the Avrami exponent, and K is an Avrami parameter depending on the geometry of the growing crystalline phase. In this model it was assumed that the material reaches 100% crystallinity. During the isothermal crystallization, heat flow (dH/dt) can be probed over crystallization time via DSC. One can derive the percent of ultimate crystallization vs time by using eq 5 and applying it to the exothermic crystallization peak:

$$X_t = \frac{\int_0^t (dH/dt)\, dt}{\int_0^\infty (dH/dt)\, dt} \tag{5}$$

In this equation, the numerator is the crystallization heat generated up to time t and the denominator is the total heat produced by the completion of the entire crystallization process. Taking the double logarithm of eq 4 gives

$$\log(-\ln(1 - X_t)) = \log K + n \log t \tag{6}$$

which suggests that $\log(-\ln(1 - X_t))$ vs $\log t$ should be linear, and K and n can be calculated by fitting a line to the experimental data. The Avrami exponent, n, is equal to the growth dimensionality plus one, and K is a function of growth geometry.

The plots of $\log(-\ln(1 - X_t))$ vs $\log t$ of PLA in the blends with different HBP contents at 112 °C are plotted in Figure 8. Each curve in Figure 8 exhibits a good linear relationship, suggesting that the isothermal crystallization kinetics was in good agreement with the Avrami equation, and the secondary crystallization was not obvious. The n, K, and $t_{1/2}$values calculated from the lines are summarized in Table 3. The Avrami exponent n varies between 2.68 and 3.20, indicating that the crystallization mode is of three-dimensional growth.[26] Crystallization half-life ($t_{1/2}$) is defined as the time at which 50% of the normalized crystallinity is reached. The larger the K and the smaller the $t_{1/2}$, the higher the crystallization rate. The data listed in Table 3 demonstrate that the incorporation of HBP increased the crystallization rate of PLA, which was consistent with the depressions of T_{cc} and T_g. In general, the crystallization kinetics of semicrystalline blend depend on effects of intermolecular interactions of the diluent amorphous phase and glass transition temperature, which is related to its chain mobility. Weak interaction and high chain mobility are favorable for the high crystallization rate.[21d] In this context, with the addition of HBP, the chain mobility and molecular interaction were both improved, and the two factors were competitive. From the above result, we can deduce that the chain mobility had a greater effect on the capacity of crystallization than the influence of H-bonding strength in this system.

Besides the plasticizing effect, we wonder whether or not the increased crystallization rate was related to the nucleating effect induced by the addition of HBP. As is well-known, when the heterogeneous nucleating agent is added to polymer, an increase in the overall crystallization rate occurs with a reduction of the nucleation induction period and an increase in the number of primary nucleation sites.[27] From POM images in Figure 9, we could find that neat PLA and its blends, irrespective of the HBP content, showed a spherulitic morphology, which was consistent with the value of Avrami exponent 3. The addition of HBP enhanced the formation of PLA crystal nucleus. With increasing the content of HBP, the nucleus density of crystallites was largely increased. Furthermore, the radius of the spherulites was dramatically reduced from more than 50 μm to about 10 μm. Small spherulites are in favor of overcoming brittleness, and as a consequence, toughness can be improved.

Phase Morphology. As is well-known, phase behavior plays a vital role in mechanical behavior of polymer blends. Already the results from DSC experiment indicated the partial miscibility of PLA/HBP blends. Further phase morphology studies can provide the relationship of the microstructure and mechanical

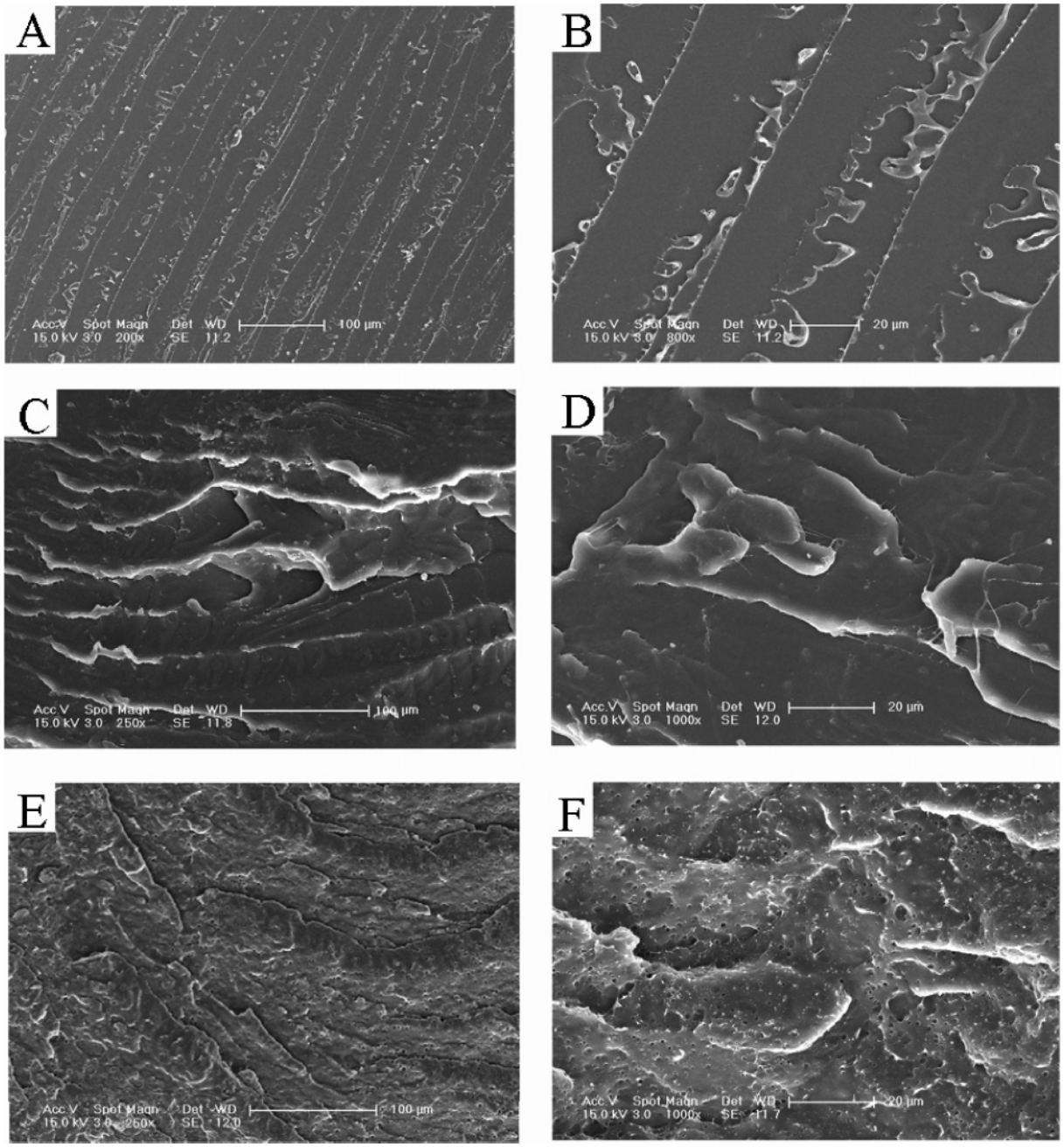

Figure 13. SEM photos of fracture surface of PLA/HBP notched-impact sample with various PLA/HBP weight compositions of (A, B) 100/0, (C, D) 90/10, and (E, F) 80/20 (the magnifications are shown).

properties.[8b] Therefore, the detailed phase morphology of PLA/HBP blends was evaluated by observation of microtomed surfaces using SEM. To enhance contrast for image analysis, the HBP phase was removed by submerging the samples in MeOH, a selective solvent for the HBP. Figure 10 shows typical SEM photos of PLA/HBP blends with various compositions (from 100/0 to 80/20). Panel A (pure PLA) shows one uniform phase, and the surface was smooth. It seems that panel B containing 2.5% HBP still displayed one phase while the phase surface was coarse. When 5.0% HBP was added, as seen in panel C, a few cavities were distinguishable, suggesting that the blend was heterogeneous, and PLA formed a continuous phase and HBP formed a dispersed phase. Also, when the HBP content was increased to 10%, small and uniform spherical cavities (diameter 0.6−0.7 μm) are clearly visible (panel D). The HBP domain had a narrow size distribution, indicating fine dispersion in the blend system. Panel E also exhibits narrow distribution cavities, but the diameter of sphere was slightly larger compared to that of panel D. Continuing to increase the HBP content resulted in agglomeration of HBP domain, and the size of HBP domain varied from 1 to 3 μm, as shown in panel F, even though the blend displayed relatively good dispersion of the HBP phase in the PLA matrix.

It has already been recognized that interfacial adhesion of blends is closely related to its miscibility.[8d,e] In our present work, the H-bonding of PLA and HBP increased with increasing the HBP content, indicating the increased interfacial adhesion. However, phase separation occurred in the blends especially for those high HBP contents, as shown by the SEM photos. It was because that not all of the OH groups in HBP were involved in H-bonding between PLA and HBP. With the increase of HBP incorporation in blend, the OH groups were prone to interact with themselves due to the stronger intramolecular hydroxyl−hydroxyl bond than the weak intermolecular hydroxyl−carbonyl

bond, leading to the aggregation of HBP. As a result, the particle diameter of HBP in blend increased with increasing HBP content.

Mechanical Properties and Toughening. Because of the absence of entanglements and the lack of crystallinity, the material obtained from neat HBP is very weak, breaks easily, and exhibits no tensile strength. Despite this fact, the mechanical properties of the blends provide desirable results. The stress−strain dependence for the blend is plotted in Figure 11, and the average values of the tensile stress and elongation at break are plotted in Figure 12. As shown in Figures 11 and 12, the neat PLA displayed no yield point, and its strain at break was only about 3.7%. On the contrary, the blends with more than 10% HBP content showed distinct yielding and stable neck growth through cold drawing. Tensile stress−strain curves indicated that fracture behavior of the specimen displayed a transition from brittle fracture to ductile fracture. Take the blend with HBP of 20% as an example; the elongation at break reached 50%, increasing by 10 times over that of neat PLA, while the yielding strength was 48.4 MPa, a slightly lower than neat PLA. Usually, toughening of a matrix material is accompanied by a drastic reduction in strength. However, the unique phenomenon of increased toughness with improved strength at some HBP contents was observed in this work. It has been demonstrated the formation of H-bonding between HBP and PLA in the above text. As is well-known, the H-bonding can enhance interfacial adhesion of polymer blends and improve the mechanical property.[16] In this context, the H-bonding increased with increasing HBP content. However, the yielding strength did not increase continuously with the increase of HBP content. It was because HBP had a lower modulus and tensile strength than PLA. When HBP content was increased beyond 5%, the stereo hindrance and dilution effects of inhomogeneous component HBP became dominant and suppressed H-bonding effect; consequently, tensile strength deteriorated. This result also coincided with the tendency of crystallinity, which first increased and then decreased. In a word, all the different contributions to tensile strength summed together explained well why an optimum in tensile strength was observed using middle concentration of HBP.

Toughness implies energy absorption and can be achieved through addition of a second phase in the form of particles. The phase-separated particles, especially after the cavitation process, induce large stress concentrations which lead to extensive shear deformation, a high-energy-absorbing mechanism.[28] The toughening effect of particles depends on their size, distribution, and particle/matrix interaction.[14] In the current work, when the HBP was added in small content, the blend was initially miscible and did not phase separate. In this case, the HBP acted as plasticizers. With increasing its content, HBP displayed finely dispersed particulate structure in PLA and toughening effect resulted. The size of HBP dispersed phase became larger as increasing the HBP concentration; however, it still remained in the range of most efficient particle diameters for dispersed phase toughened composites, which was reported to range between 500 nm and 10 μm.[29]

To further study the toughening effect of PLA/HBP blends, the fracture surface of the impact specimen was investigated by SEM. As shown in Figure 13, SEM photos of the impact-fractured surfaces showed more evidence of brittle−ductile transition with the addition of HBP. In Figure 13A,B, neat PLA showed a very smooth surface with groups of parallel lines, indicating a typical brittle fracture behavior. On the fracture surfaces of PLA with 10% HBP (Figure 13 C,D), multiple fracture surfaces replaced the single fracture lines. Some fibrils were discernible on the fracture surfaces. The toughening effect in this case remained moderate. When HBP was increased to 20% (Figure 13E,F), the surfaces become increasingly rough, with more threads found. Furthermore, oval cavities were visible and the matrix around the cavity underwent some deformation, inducing a favorable toughening effect. These cavities were formed during impact when the stress was higher than the bonding strength at the interface between the PLA matrix and HBP inclusions. With the debonding progress, PLA matrix between HBP particles deformed more easily to achieve the shear yielding and thus thoughen.

It is well recognized that a strong interfacial adhesion usually results in low toughness as it does not allow the stress to be relieved via interfacial debonding. However, low interfacial adhesion inducing immiscibility or totally phase segregation is not favor for the tensile strength. In this work, improved toughness was achieved, and at the same time, the tensile strength was not detrimentally compromised. Accordingly, we believe that an ideally good interfacial adhesion via hydrogen bonding between PLA and HBP is obtained, so that a good balance of the mechanical properties of the blend is achieved.

4. Conclusions

The aim of this study was to obtain a plasticizing or toughening effect of PLA without sacrificing the processability, thermal properties, and mechanical strength. It was achieved by using hyperbranched poly(ester amide) as modifier. The effect of hyperbranched polymer as a processing aid on PLA was visible from the rheological measurement. It showed that adding a small amount of HBP (2.5%) resulted in a dramatic reduction of the complex viscosity of PLA. The slight depression of T_g with the increase of HBP content indicated partial miscibility of the blend system, which was resulted from the H-bonding between carbonyl of PLA with hydroxyl and amine of HBP. Meanwhile, the HBP component acted as a heterogeneous nucleating agent and improved the crystallization capability of PLA. Remarkably, with the addition of HBP, the failure mode changed from brittle fracture of the neat PLA to ductile fracture of the blend as demonstrated by tensile test and fracture surface microgram. The elongation at break of the blend was improved by more than 10 times compared to the neat PLA, using 20 wt % HBP. Surprisingly, the blend showed increased yielding strength within 10% content of HBP. The H-bonding and increased crystallinity were considered to be responsible for the enhanced yielding strength. HBP modifier, forming a finely dispersed particulate structure in PLA, functioned as stress concentrators undergo cavitation via debonding. The moderate interfacial bonding was involved in the toughening of the blend. In summary, the hyperbranched poly(ester amide) did afford an advantage in processability and thermal and mechanical properties of PLA. To our best knowledge, until now, no other modifier for PLA could meet the challenge of property improvement without drastic loss of the general performance. We believe it helpful for developing high-performance PLA.

Acknowledgment. The authors are grateful for subsidy by the National Natural Science Foundation of China (Nos. 50473027 and 50525312).

References and Notes

(1) (a) Lunt, J. *Polym. Degrad. Stab.* **1998**, *59*, 145. (b) Jacobsen, S.; Degee, Ph.; Fritz, H. G.; Dubois, Ph.; Jerome, R. *Polym. Eng. Sci.* **1999**, *39*, 1311. (c) Drumright, R. E.; Gruber, P. R.; Henton, D. E.

Adv. Mater. **2000**, *12*, 1841. (d) Kikkawa, Y.; Abe, H.; Iwata, T.; Doi, Y. *Biomacromolecules* **2001**, *2*, 940.
(2) Cai, H.; Dave, V.; Gross, R. A.; McCathy, S. P. *J. Polym. Sci., Part B: Polym. Phys.* **1996**, *40*, 2701.
(3) (a) Lenz, R. W. *Adv. Polym. Sci.* **1994**, *112*, 1. (b) Deng, C.; Tian, H.; Zhang, P.; Sun, J.; Chen, X.; Jing, X. *Biomacromolecules* **2006**, *7*, 590. (c) Hanefeld, P.; Westedt, U.; Wombacher, R.; Kissel, T.; Schaper, A.; Wendorff, J. H.; Greiner, A. *Biomacromolecules* **2006**, *7*, 2086. (d) Bailey, T. S.; Rzayev, J.; Hillmyer, M. A. *Macromolecules* **2006**, *39*, 8772.
(4) (a) Dell'Erba, R.; Groeninckx, G.; Maglio, G.; Malinconico, M.; Migliozzi, A. *Polymer* **2001**, *42*, 7831. (b) Na, Y. H.; He, Y.; Shuai, X. T.; Kikkawa, Y.; Doi, Y.; Inoue, Y. *Biomacromolecules* **2002**, *3*, 1179. (c) Choi, N. S.; Kim, C. H.; Cho, K. Y.; Park, J. K. *J. Appl. Polym. Sci.* **2002**, *86*, 1892.
(5) (a) Hu, Y.; Rogunova, M.; Topolkaraev, V.; Hiltner, A.; Baer, E. *Polymer* **2003**, *44*, 5701. (b) Zhang, K.; Simon, C. G., Jr.; Washburn, N. R.; Antonucci, J. M.; Lin-Gibson, S. *Biomacromolecules* **2005**, *6*, 1615. (c) Kulinski, Z.; Piorkowska, E. *Polymer* **2005**, *46*, 10290.
(6) (a) Kulinski, Z.; Piorkowska, E.; Gadzinowska, K.; Stasiak, M. *Biomacromolecules* **2006**, *7*, 2128. (b) Piorkowska, E.; Kulinski, Z.; Galeski, A.; Masirek, R. *Polymer* **2006**, *47*, 7178.
(7) (a) Ferreira, B. M. P.; Zavaglia, C. A. C.; Duek, E. A. R. *J. Appl. Polym. Sci.* **2002**, *86*, 2898. (b) Focarete, M. L.; Scandola, M.; Dobrzynski, P.; Kowalczuk, M. *Macromolecules* **2002**, *35*, 8472. (c) Koyama, N.; Doi, Y. *Macromolecules* **1996**, *29*, 5843. (d) Koyama, N.; Doi, Y. *Polymer* **1997**, *38*, 1589. (e) Zhang, L. L.; Xiong, C. D.; Deng, X. M. *Polymer* **1996**, *37*, 235.
(8) (a) Wang, H.; Sun, X. Z.; Seib, P. *J. Appl. Polym. Sci.* **2001**, *82*, 1761. (b) Wang, H.; Sun, X. Z.; Seib, P. *J. Appl. Polym. Sci.* **2003**, *90*, 3683. (c) Zhang, J. F.; Sun, X. Z. *Biomacromolecules* **2004**, *5*, 1446. (d) Jiang, L.; Wolcott, M. P.; Zhang, J. *Biomacromolecules* **2006**, *7*, 199. (e) Zhang, J. W.; Jiang, L.; Zhu, L. Y.; Jane, J.-L.; Mungara, P. *Biomacromolecules* **2006**, *7*, 1551.
(9) (a) Ljungberg, N.; Wesslen, B. *Biomacromolecules* **2005**, *6*, 1789. (b) Martin, O.; Averous, L. *Polymer* **2001**, *42*, 6209.
(10) (a) Fréchet, J. M. J.; Tomalia, D. A. *Dendrimers and Other Dendritic Polymers*; Wiley: Chichester, England, 2002. (b) Kim, Y. H. *J. Polym. Sci., Part A: Polym. Chem.* **1998**, *36*, 1685. (c) Voit, B. *J. Polym. Sci., Part A: Polym. Chem.* **2000**, *38*, 2505. (d) Inoue, K. *Prog. Polym. Sci.* **2000**, *25*, 453. (e) Jikei, M.; Kakimoto, M. *J. Polym. Sci., Part A: Polym. Chem.* **2004**, *42*, 1293. (f) Gao, C.; Yan, D. *Prog. Polym. Sci.* **2004**, *29*, 183. (g) Voit, B. *J. Polym. Sci., Part A: Polym. Chem.* **2005**, *43*, 2679.
(11) Flory, P. J. In *Principles of Polymer Chemistry*; Cornell University Press: Ithaca, NY, 1952; Chapter 9.
(12) (a) Kim, Y. H.; Webster, O. W. *J. Am. Chem. Soc.* **1990**, *112*, 4592. (b) Kim, Y. H.; Webster, O. W. *Macromolecules* **1992**, *25*, 5561−5572. (c) Voit, B. I. *Acta Polym.* **1995**, *46*, 87. (d) Schmaljohann, D.; Pötschke, P.; Hässler, R.; Voit, B. I.; Froehling, P. E.; Mostert, B.; Loontjens, J. A. *Macromolecules* **1999**, *32*, 6333. (e) Nunez, C. M.; Chiou, B.-S.; Andrady, A. L.; Khan, S. A. *Macromolecules* **2000**, *33*, 1720.
(13) (a) Hong, Y.; Cooper-White, J. J.; Mackay, M. E.; Hawker, C. J.; Malmström, E.; Rehnberg, N. *J. Rheol.* **1991**, *43*, 781−793. (b) Hong, Y.; Coombs, S. J.; Cooper-White, J. J.; Mackay, M. E.; Hawker, C. J.; Malmström, E.; Rehnberg, N. *Polymer* **2000**, *41*, 7705.
(14) (a) Boogh, L.; Pettersson, B.; Månson, J.-A. E. *Polymer* **1999**, *40*, 2249. (b) Mezzenga, R.; Boogh, L.; Månson, J.-A. E. *Compos. Sci. Technol.* **2001**, *61*, 787. (c) Mezzenga, R.; Plummer, C. J. G.; Boogh, L.; Månson, J.-A. E. *Polymer* **2001**, *42*, 305. (d) Mezzenga, R.; Månson, J.-A. E. *J. Mater. Sci.* **2001**, *36*, 4883. (e) Mezzenga, R.; Boogh, L.; Pettersson, B.; Månson, J.-A. E. *Macromol. Symp.* **2000**, *149*, 17. (f) Fröhlich, J.; Kautz, H.; Thomann, R.; Frey, H.; Mülhaupt, R. *Polymer* **2004**, *45*, 2155.
(15) (a) Johansson, M.; Hult, A. *J. Coat. Technol.* **1995**, *67*, 35. (b) Schmaljohann, D.; Voit, B. I.; Jansen, J. F. G. A.; Hendriks, P.; Loontjens, J. A. *Macromol. Mater. Eng.* **2000**, *275*, 31.
(16) (a) Massa, D. J.; Shriner, K. A.; Turner, S. R.; Voit, B. *Macromolecules* **1995**, *28*, 3214. (b) Huber, T.; Pötschke, P.; Pompe, G.; Hässler, R.; Voit, B.; Grutke, S.; Gruber, F. *Macromol. Mater. Eng.* **2000**, *280/281*, 33. (c) Monticelli, O.; Oliva, D.; Russo, D.; Clausnitzer, C.; Pötschke, P.; Voit, B. *Macromol. Mater. Eng.* **2003**, *288*, 318.
(17) (a) Li, X. R.; Zhan, J.; Li, Y. S. *Macromolecules* **2004**, *37*, 7584. (b) Li, X. R.; Zhan, J.; Lin, Y.; Li, Y. S. *Macromolecules* **2005**, *38*, 8235. (c) Li, X. R.; Lu, X. F.; Lin, Y.; Zhan, J.; Li, Y. S.; Liu, Z. Q.; Chen, X. S.; Liu, S. Y. *Macromolecules* **2006**, *39*, 7889.
(18) Li, X. R.; Su, Y. L.; Chen, Q. Y.; Lin, Y.; Tong, Y. J.; Li, Y. S. *Biomacromolecules* **2005**, *6*, 3181.
(19) Sarasua, J. R.; Prud'homme, R. E.; Wisniewski, M.; Le, Borgne, A.; Spassky, N. *Macromolecules* **1998**, *31*, 3895.
(20) Fox, T. G. *J. Appl. Bull. Am. Phys. Soc.* **1956**, *1*, 123.
(21) (a) Mikhaylova, Y.; Adam, G.; Häussler, L.; Eichhorn, K. J.; Voit, B. *J. Mol. Struct.* **2006**, *788*, 80. (b) Viswanathan, S.; Dadmun, M. D. *Macromolecules* **2002**, *35*, 5049. (c) Kuo, S. W.; Chan, S. C.; Wu, H. D.; Chang, F. C. *Macromolecules* **2005**, *38*, 4729. (d) Kuo, S. W.; Chan, S. C.; Chang, F. C. *Macromolecules* **2003**, *36*, 6653.
(22) Coleman, M. M.; Graf, J. F.; Painter, P. C. *Specific Interactions and the Miscibility of Polymer Blends*; Technomic: Lancaster, PA, 1991.
(23) (a) Eling, B.; Gogolewski, S.; Pennings, A. J. *Polymer* **1982**, *23*, 1587. (b) Puiggali, J.; Ikada, Y.; Tsuji, H.; Cartier, L.; Okihara, T.; Lotz, B. *Polymer* **2000**, *41*, 8921.
(24) Wong, S.; Shanks, R. A.; Hodzic, A. *Macromol. Mater. Eng.* **2004**, *289*, 447−456.
(25) Avrami, M. *J. Chem. Phys.* **1939**, *7*, 1103; **1940**, *8*, 212; **1941**, *9*, 177.
(26) Cyras, V. P.; Kenny, J. M.; Vazquez, A. *Polym. Eng. Sci.* **2001**, *41*, 1521.
(27) Schmidt, S. C.; Hillmyer, M. A. *J. Polym. Sci., Part B: Polym. Phys.* **2001**, *39*, 300.
(28) (a) Wu, J. S.; Yee, A. F.; Mai, Y. W. *J. Mater. Sci.* **1994**, *29*, 4510. (b) Kim, G. M.; Michler, G. H. *Polymer* **1998**, *39*, 5699.
(29) Pascault, J. P.; Sautereau, H.; Verdu, J.; Williams, R. J. J. *Thermosetting Polymers*; Marcel Dekker: New York, 2002.

MA070989A